Solute Dispersion in Casson Blood Flow through a Stenosed Artery with the Effect of Magnetic Field

Nur Husna Amierah Mohd Zaperi[1], Nurul Aini Jaafar[1,*]

[1] Department of Mathematical Sciences, Faculty of Science, Universiti Teknologi Malaysia, 81310 Johor Bahru, Johor, Malaysia

ARTICLE INFO	ABSTRACT
	Individuals with atherosclerosis cardiovascular disease (aCVD) have a higher risk of cancer than those without aCVD. In chemotherapy, the drug injected into the blood vessels that treat cancer by attacking cells at a specific site in an organ allows better treatment for cancer. One of the most important strategies for directing medication to the site of the cancer is magnetic drug administration such as neodymium magnets treatment. Magnetic drug targeting can reduce the side effects of drugs and optimize magnetic field to speed up treatment. Hence, this study examines the steady solute dispersion in blood flow through a stenosed artery with the effect of magnetic field by using Casson fluid model. The momentum and constitutive equations are solved analytically using integration to obtain the velocity of blood flow. The convective diffusion equation is solved by applying generalized dispersion model (GDM) and integration to obtain steady and unsteady dispersion functions and overall dispersion function. The effects of magnetic field and height of stenosis on the blood flow and solute dispersion are investigated. The results are validated with the previous solution without the effect of magnetic field and height of stenosis. The results showed a good conformity between the two solutions. An increase in magnetic field increase the velocity and steady dispersion function while reducing the unsteady dispersion function and overall dispersion function. However, when the height of stenosis is considered in the problem, it behaves differently for velocity, steady and unsteady dispersion functions and overall dispersion function. It is observed that the solute dispersion in blood flow is affected by magnetic field. The results of the presence study can potentially be used to predict the changes of blood flow behaviour and dispersion process in blood flow. In conclusion, the use of magnetic fields in magnetic therapy aids the body to reduce muscular inflammation and pain. Magnetic field affect the solute dispersion in human blood flow.

1. Introduction

Cardiovascular disease (CVD) and cancer are leading causes of death with the inclined number of the elderly population and early cancer screening and treatment, the number of cancers cases are rising, while the mortality rate is decreasing [21]. CVD and cancer share several risk factors such as unhealthy diet, tobacco use and harmful use of alcohol. According to Bell *et al.,* [4], individuals with atherosclerosis CVD (aCVD) had a higher risk of cancer than those without CVD. Cancer subtype

---

analysed specific associations of aCVD with several malignancies including lung, bladder, liver, colon and other hematologic cancer. Cancer has several treatments such as surgery, chemotherapy, radiation therapy and targeted drug delivery.

In chemotherapy, specific medications are used to kill fast-growing cancerous cells [3]. Treatment success depends on delivering a sufficient amount of medicine to tumor cells when keeping damage to healthy cells at the minimum tolerable level [3]. Generally, delivering the right amount of medicine to human body is a crucial factor in curing many diseases. Therefore, it is desirable to develop chemotherapeutics that can either passively or actively target cancerous cells, thereby reducing adverse side effects while improving therapeutic efficacy [13]. Thus, to improve the chemotherapy treatment, it is important to understand the drug process in human body. For this reason, it helps to improve the survival rate of cancer patients [20].

One of the most important strategies for directing medication to the site of the tumor is magnetic drug administration such as neodymium magnets treatment. Magnetic drug targeting can reduce the side effects of drugs and optimize magnetic field to speed up treatment. By overcoming these constraints, a large number of pharmacological agents may be delivered into a controlled area of the body with few undesirable side effects [10]. One of the problems of successful magnetic drug targeting is controlling the accumulation of magnetic nanoparticles in the human body and aiming deeper tissues using an electromagnet's external magnetic field [18]. Human body experiences magnetic fields of moderate to high intensity in many situations of day-to-day life. Nowadays, magnetic therapy is frequently used to treat a variety of diseases. The use of magnetic fields in magnetic therapy aids the body to reduce muscular inflammation and pain. Magnetic field may affect the solute dispersion in human blood flow.

The solute transportation in blood flow was studied and very important in transferring drugs into the physiological system. The problem of solute dispersion process in blood flow getting more important and it has more widely studied by researchers. Investigating the solute dispersion in blood flow is crucial for better treatment of cancer. In the study conducted by Taylor [16], the research focused on the phenomenon of solute dispersion inside a solvent in a linear pipe under conditions of steady flow. The solute exhibits diffusion because of the interaction between molecule diffusion and velocity variance throughout its cross-sectional area, resulting in the solute diffusing with molecular diffusivity, $\bar{D}_{eff} = \bar{a}^2 \bar{u}_m^2 / 48 \bar{D}_m$ where $\bar{a}$ is pipe radius, $\bar{u}_m$ is mean velocity and $\bar{D}_m$ is molecular diffusivity.

The solute dispersion theory of Taylor showed by Aris [2] is only valid when $\bar{D}_{eff} > \bar{D}_m$. Then, Aris [2] introduced the Taylor-Aris dispersion method, which describes the impact of axial molecule diffusion. The latter theory was only viable for a limited time. The work of Taylor-Aris has been simplified by Gill [7] by the establishment of a distribution for the local concentration, which is derived from a series expansion based on the mean concentration and is applicable for all time periods. Then, Gill and Sankarasubramanian [8] developed the first GDM to analyze the solute dispersion process. Sankarasubramanian and Gill [12] explored scattering in the presence of a wall response using exchange, convection, and scattering coefficients.

Casson fluid is one of the useful and important fluid models to investigate the blood viscosity and yield stress. Das *et al.,* [5] investigated the solute dispersion in blood flow through a constricted artery with an absorptive wall using Casson fluid model and has been solved using convective diffusion equation. Ali *et al.,* [1] investigated non-Newtonian of Casson fluid with the pulsation in a channel having symmetrical constriction bumps on the upper and lower walls. The mathematical model has been solved by using vorticity-stream function form. Jamil *et al.,* [9] analysed the Casson fluid of magnetic blood flow in an inclined stenosed artery and has been solved by using Caputo Fabrizio

fractional derivative without singular kernel. Shahzad *et al.,* [14] investigated the fluid structure interaction study using Casson fluid in a bifurcated channel having stenosis with elastic wall and has been solved by using Arbitrary Lagrangian-Eulerian (ALE).

All the above work based on the constant viscosity model of the fluid in blood flow. Several authors studied the solute dispersion in blood flow with the effect of magnetic field. Recently, Priyadharshini and Ponalagusamy [11] analysed the magnetohydrodynamics effects on flow parameters of blood carrying magnetic nanoparticles flowing through a stenosed artery with the effect of magnetic field and body acceleration and has been solved by using finite difference schemes. Suneetha *et al.,* [15] investigated the theoretical analysis of Casson fluid with the hybrid magnetic nanoparticles as drug carrier with the magnetic field and has been solved by using Runge-Kutta method. Yadeta and Shaw [22] investigated the efficiency of the magnetic drug capture at tumor region using Casson fluid model and the solution has been analytical solved by using Caputo fractional order time-derivative. This clearly indicated that the effect of magnetic field may be significantly affected the blood flow.

The present work is devoted to study the solute dispersion in blood flow through stenosed artery with the effect of magnetic field by using Casson fluid model. The momentum and constitutive equations have been solved analytically by using integral method to obtain the velocity of blood flow. The obtained velocity has been used to get the steady and unsteady dispersion functions and overall dispersion function by solving the convective-diffusion equation using generalized dispersion model (GDM). The study may help to understand the physiological processes of the injection of drug in the bloodstream when the magnetic field exists in stenosed artery.

2. Methodology
2.1 Mathematical Formulation

Consider the flow of the blood assumed as viscous incompressible fluid through a circular pipe in a laminar, continuous, axisymmetric and fully formed unidirectional flow in the axial direction, treating blood as Casson fluid model. The pipe flow geometry describes the artery with the presence of magnetic field are shown in Figure 1, where $\bar{L}$ is the length of conduit, R_0 is the artery's radius, $\bar{\psi}$ is the azimuthal angle, $\bar{r}_p$ is the radius of the plug region in circular pipe, $\bar{\delta}$ is stenosis height, $\bar{u}$ is the velocity of fluid flow, M is magnetic field and $\bar{z}$ is the axial coordinate for circular pipe.
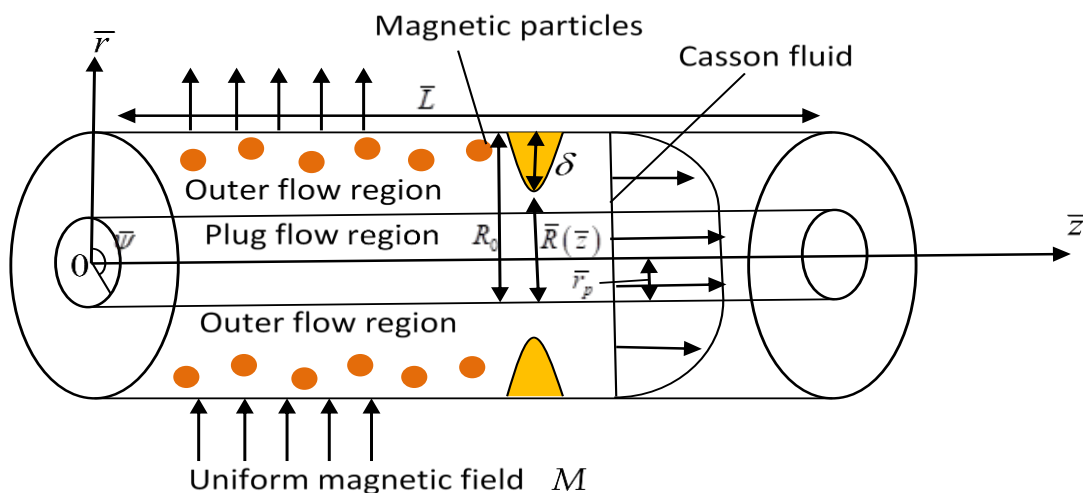

Fig. 1. Pipe flow geometry of Casson fluid model with the influenced of magnetic field

2.2 Governing Equation

The momentum equation which governs the flow is given as follows [17]:

$$\frac{1}{\bar{r}}\frac{d}{d\bar{r}}(\bar{r}\bar{\tau}) - \frac{d\bar{p}}{d\bar{z}} + \mu_0 M \frac{d\bar{H}}{d\bar{z}} = 0, \tag{1}$$

where the variables of $\bar{\tau}$, $\bar{p}$, μ_0, M, and $d\bar{H}/d\bar{z}$ are the shear stress, the fluid pressure, the fluid density, the magnetic permeability of the vacuum, the magnetic field and the magnetic field gradient. The boundary condition for momentum equation is given as

$$\bar{\tau} = \text{finite at } \bar{r} = 0. \tag{2}$$

The constitutive equation is defined as

$$-\frac{d\bar{u}}{d\bar{r}} = \begin{cases} \frac{1}{\mu}\left(\sqrt{\bar{\tau}} - \sqrt{\bar{\tau}_y}\right)^2 & \text{if } \bar{\tau} > \bar{\tau}_y, \\ 0 & \text{if } \bar{\tau} \leq \bar{\tau}_y, \end{cases} \tag{3}$$

where $\bar{u}$, $\bar{\tau}_y$, μ are the velocity of the fluid flow, the yield stress and the coefficient of viscosity for the Casson fluid model. The slip boundary condition for constitutive equation is given by Verma *et al.,* [19]

$$\bar{u} = \bar{u}_s \text{ at } \bar{r} = \bar{R}(\bar{z}), \tag{4}$$

where

$$\bar{R}(\bar{z}) = R_0\left(1 - \frac{\bar{\delta}}{R_0}\exp\left(-\frac{\bar{k}^2\bar{\varepsilon}^2\bar{z}^2}{R_0^2}\right)\right), \tag{5}$$

where $\bar{R}(\bar{z})$ is the stenosed segment's radius, $\bar{\delta}$ is the stenosis height at the central point and $\bar{k}$ is the constant in parameters and radius, $\bar{\varepsilon} = R_0/\bar{L}_0$. Consider the geometry of stenosis in Figure 1 in Eq. (5) as below

$$\frac{\bar{R}(\bar{z})}{R_0} = 1 - ae^{-bz^2}, \tag{6}$$

where $a = \bar{\delta}/R_0$ and $b = \bar{k}^2\bar{\varepsilon}^2/R_0^2$ are the variables in $\bar{R}(\bar{z})$. Non-dimensional for Eq. (6) as below

$$R(z) = 1 - a_1 e^{(-b_1 z^2)}, \tag{7}$$

where $a_1 = \delta$ and $b_1 = bR_0^2$ are variables in $R(z)$. The mean velocity is given as follows

$$\bar{u}_m = \frac{2}{\bar{R}^2(\bar{z})}\left[\int_0^{\bar{r}_p} \bar{u}(\bar{r}_p)\bar{r}d\bar{r} + \int_{\bar{r}_p}^{\bar{R}(\bar{z})} \bar{u}(\bar{r})\bar{r}d\bar{r}\right]. \tag{8}$$

Then, two-dimensional unsteady convective-diffusion equation is expressed as follows:

$$\frac{\partial \bar{C}}{\partial \bar{t}} + u\frac{\partial \bar{C}}{\partial \bar{z}^*} = \bar{D}_m\left(\frac{1}{\bar{r}}\frac{\partial}{\partial \bar{r}}\left(\bar{r}\frac{\partial}{\partial \bar{r}}\right) + \frac{\partial^2}{\partial \bar{z}^{*2}}\right)\bar{C}. \tag{9}$$

Simplify Eq. (9), it yields

$$\frac{\partial \bar{C}}{\partial \bar{t}} + \bar{u}\frac{\partial \bar{C}}{\partial \bar{z}^*} = \bar{D}_m\left(\ell^2 + \frac{\partial^2}{\partial \bar{z}^{*2}}\right)\bar{C}, \tag{10}$$

where

$$\ell^2 = \frac{1}{\bar{r}}\frac{\partial}{\partial \bar{r}}\left(\bar{r}\frac{\partial}{\partial \bar{r}}\right). \tag{11}$$

According to Gill and Sankarasubramanian [8], the initial condition of convective diffusion coefficient is given by

$$\bar{C}(\bar{r},\bar{z},0) = \begin{cases} C_0 \text{ if } |\bar{z}| \le \dfrac{\bar{z}_s}{2}, \\ 0 \text{ if } |\bar{z}| > \dfrac{\bar{z}_s}{2}, \end{cases} \tag{12}$$

where C_0 is the concentration referenced and $\bar{z}_s$ is the solute's length. The boundary condition following Gill and Sankarasubramanian [8] is

$$\bar{C}(\bar{r},\infty,\bar{t}) = 0, \tag{13}$$

for symmetry at the central circular pipe $\bar{r} = 0$, the boundary condition is

$$\frac{\partial \bar{C}}{\partial \bar{r}}(0,\bar{z},\bar{t}) = 0 \tag{14}$$

and for the solute concentration gradient at the wall $\bar{r} = \bar{R}(\bar{z})$, the boundary condition is given by

$$\frac{\partial \bar{C}}{\partial \bar{r}}(\bar{R}(\bar{z}),\bar{z},\bar{t}) = 0. \tag{15}$$

2.3 Non-dimensional Variables

The non-dimensional variables are as follows:

$$r = \frac{\bar{r}}{R_0}, \; \tau = \frac{\bar{\tau}R_0}{\bar{\mu}u_0}, \; p = \frac{\bar{p}\bar{\mu}u_0}{R_0}, \; z = \frac{\bar{z}}{R_0}, \; u = \frac{\bar{u}}{u_0}, \; \tau_y = \frac{\bar{\tau}_y R_0}{\bar{\mu}u_0}, \; u_s = \frac{\bar{u}_s}{u_0}, \; R(z) = \frac{\bar{R}(z)}{R_0},$$

$$r_p = \frac{\bar{r}_0}{R_0}, \; H = \frac{\bar{H}}{H_0}, \; C = \frac{\bar{C}}{C_0}, \; z^* = \frac{\bar{D}_m \bar{z}^*}{R_0^2 u_0}, \; z_s = \frac{\bar{D}_m \bar{z}_s}{R_0^2 u_0}, \; t = \frac{\bar{D}_m \bar{t}}{\bar{a}^2}, \tag{16}$$

where u_0, r, τ, p, R_0, z/z^*, u, τ_y, u_s, $R(z)$, r_p, C, z_s, H and t are the fluid characteristic velocity, the radial coordinate, the shear stress, the pressure gradient, the radius of artery in outer region, the radial direction, the velocity, the yield stress, the slip velocity, the stenosed radius respectively in non-dimensional variables, the radius of artery in plug flow region, the solute concentration, the solute length, the magnetic field intensity and the time.

2.4 Solution of Governing Equation

The momentum equation in Eq. (1) is substituted with Eq. (16) and it forms a non-dimensional of momentum equation which is given as follows

$$\frac{1}{r}\frac{d}{dr}(r\tau) = -B\frac{dH}{dz} + \frac{dp}{dz}, \tag{17}$$

where $B = \dfrac{\mu_0 M H_0 a}{u\mu}$. Then, Eq. (17) is solved by using integration of r and it becomes

$$\tau = \frac{r}{2}\left(-B\frac{dH}{dz} + \frac{dp}{dz}\right) + C_1, \tag{18}$$

where C_1 is a constant integration. The boundary equation of momentum equation in Eq. (2) then being applied with non-dimensional in Eq. (16), it forms

$$\tau = \text{finite at } r = 0. \tag{19}$$

Applying non-dimensional boundary equation of momentum equation in Eq. (19) into Eq. (18), it is given as

$$\tau = \frac{r}{2}\left(-B\frac{dH}{dz} + \frac{dp}{dz}\right). \tag{20}$$

To form the yield stress, $\tau = \tau_y$ and $r = r_p$ are applied into Eq. (20), it forms

$$\tau_y = \frac{r_p}{2}\left(-B\frac{dH}{dz} + \frac{dp}{dz}\right). \tag{21}$$

Then, the constitutive equation of Casson fluid in Eq. (3) is substituted with Eq. (16) to forms non-dimensional constitutive equation which given as below

$$-\frac{du}{dr} = \tau + \tau_y - 2\sqrt{\tau}\sqrt{\tau_y}. \tag{22}$$

Both Eq. (20) and (21) are substituted into Eq. (22), it forms

$$-\frac{du}{dr} = \left(\frac{r}{2}\left(-B\frac{dH}{dz}+\frac{dp}{dz}\right)\right) + \left(\frac{r_p}{2}\left(-B\frac{dH}{dz}+\frac{dp}{dz}\right)\right) - 2\sqrt{\left(\frac{r}{2}\left(-B\frac{dH}{dz}+\frac{dp}{dz}\right)\right)}\sqrt{\left(\frac{r_p}{2}\left(-B\frac{dH}{dz}+\frac{dp}{dz}\right)\right)}. \tag{23}$$

Then, the Eq. (23) is solved using integration of r and it forms

$$-u(r) = \frac{1}{2}\left(-B\frac{dH}{dz}+\frac{dp}{dz}\right)\left(\frac{r^2}{2}+rr_p-\frac{4\sqrt{r_p}r^{\frac{3}{2}}}{3}\right)+C_2, \tag{24}$$

where C_2 is also a constant integration. The non-dimensional of boundary equation for constitutive equation is forms by substituting Eq. (16) into Eq. (4), it yields

$$u = u_s \text{ at } r = R(z). \tag{25}$$

By substituting Eq. (25) into Eq. (24), it forms

$$C_2 = -u_s - \frac{1}{2}\left(-B\frac{dH}{dz}+\frac{dp}{dz}\right)\left(\frac{R(z)^2}{2}+R(z)r_p-\frac{4\sqrt{r_p}R(z)^{\frac{3}{2}}}{3}\right). \tag{26}$$

Eq. (26) is then substituted into Eq. (24), it forms the velocity in the outer non-plug core which is given as follows

$$u(r) = -\frac{1}{2}\left(-B\frac{dH}{dz}+\frac{dp}{dz}\right)\left(\frac{r^2}{2}+rr_p-\frac{4\sqrt{r_p}r^{\frac{3}{2}}}{3}\right)+\frac{1}{2}\left(-B\frac{dH}{dz}+\frac{dp}{dz}\right)\left(\frac{R(z)^2}{2}+R(z)r_p-\frac{4\sqrt{r_p}R(z)^{\frac{3}{2}}}{3}\right) \tag{27}$$

$$+u_s.$$

Then, $r = r_p$ is applied into Eq. (27) which forms the velocity in plug flow region,

$$u(r_p) = -\frac{1}{2}\left(-B\frac{dH}{dz}+\frac{dp}{dz}\right)\left(\frac{r_p^2}{2}+r_p^2-\frac{4r_p^2}{3}\right)+\frac{1}{2}\left(-B\frac{dH}{dz}+\frac{dp}{dz}\right)\left(\frac{R(z)^2}{2}+R(z)r_p-\frac{4\sqrt{r_p}R(z)^{\frac{3}{2}}}{3}\right) \tag{28}$$

$$+u_s.$$

By substituting Eq. (16) into Eq. (10), it is given as

$$\frac{\partial C}{\partial t} + u \frac{\partial C}{\partial z^*} = \left(\ell^2 + \frac{1}{Pe^2} \frac{\partial^2}{\partial z^{*2}} \right) C, \tag{29}$$

where

$$Pe = \frac{R_0 u_0}{D_m}. \tag{30}$$

Here, Pe is the Peclet number for the flow in a circular pipe which is given by Dash *et al.,* [6]. By using approach of Sankarasubramanian and Gill [12] and by assuming the solution of Eq. (29) as a derivative series expansion involving $\partial^i C_m / \partial z_1^i$ is shown as follows:

$$C(r,z,t) = C_m(z_1,t) + \sum_{i=1}^{\infty} f_i(r,t) \frac{\partial^i C_m(z_1,t)}{\partial z_1^i}, \tag{31}$$

where C_m is the mean concentration of the solute over a cross-sectional area of the geometry, $f_i(r,t)$ is the dispersion function associated with $\partial^i C_m / \partial z_1^i$. By substituting Eq. (16) into Eq. (12) - Eq. (15), the non-dimensional of initial and boundary conditions of convective-diffusion equation are given as

$$C(r,z,0) = \begin{cases} 1 \text{ if } |z| \leq \dfrac{z_s}{2}, \\ 0 \text{ if } |z| > \dfrac{z_s}{2}, \end{cases} \tag{32}$$

$$C(r,\infty,t) = 0, \tag{33}$$

$$\frac{\partial C}{\partial r}(0,z,t) = 0, \tag{34}$$

and

$$\frac{\partial C}{\partial r}(R(z),z,t) = 0. \tag{35}$$

Using the initial condition Eq. (32) into Eq. (37), it yields $f_0(r,0) = 1$. Multiplying the solution in Eq. (37) with r and integrating it from 0 to $R(z)$ with the respect to r, it forms

$$C_m(z_1,t) = 2 \int_0^{R(z)} C(r,z_1,t) r dr. \tag{36}$$

According to Sankarasubramanian and Gill [12], the GDM is a derivative series expansion which given as

$$\frac{\partial C_m}{\partial t}(z_1,t) = \sum_{i=1}^{\infty} K_i(t)\frac{\partial^i C_m}{\partial z_1^i}(z_1,t),$$

(37)

where $K_i(t)$ is the transport coefficient. The mean velocity plays an important role in calculating dispersion function. Thus, Eq. (16) is substituted into Eq. (8), the non-dimensional of mean velocity is given as below

$$u_m = \frac{2}{R^2(z)}\left[\int_0^{r_p} u(r_p)rdr + \int_{r_p}^{R(z)} u(r)rdr\right].$$

(38)

Then, the mean velocity is solved by using integration of r, it forms

$$u_m = \frac{1}{8}\left(-B\frac{dH}{dz}+\frac{dp}{dz}\right)\left(R^2(z)+\frac{4}{3}r_p R(z)-\frac{16}{7}\sqrt{r_p}R^{\frac{3}{2}}(z)-\frac{1}{21}\frac{r_p^4}{R^2(z)}\right)+u_s.$$

(39)

The dispersion function at steady state is given by

$$\frac{1}{r}\frac{\partial}{\partial r}\left(r\frac{\partial f_{1s_-}}{\partial r}\right)-\left(u(r_p)-u_m\right)=0 \text{ if } 0\le r\le r_p$$

(40)

and the dispersion function in outer region is given as follows:

$$\frac{1}{r}\frac{\partial}{\partial r}\left(r\frac{\partial f_{1s_+}}{\partial r}\right)-\left(u(r)-u_m\right)=0 \text{ if } r_p\le r\le R(z).$$

(41)

Eq. (40) and Eq. (41) are solved by using integral method to get f_{1s_-} and f_{1s_+}

$$\frac{df_{1s}}{dr}(0)=0$$

(42)

and

$$\frac{df_{1s}}{dr}R(z)=0.$$

(43)

The steady dispersion function in the plug flow region, f_{1s_-} and outer flow region, f_{1s_+}. Thus, the steady dispersion function in the plug flow region, f_{1s_-} yields

$$f_{1s_-} = CI - \frac{Ar^2 r_p^2}{48} + \frac{Ar^2 r_p^4}{672R^2(z)} + \frac{1}{12}Ar^2 r_p R(z) - \frac{2}{21}Ar^2 \sqrt{r_p} R^{\frac{3}{2}}(z) + \frac{1}{32}Ar^2 R^2(z) \qquad (44)$$

and outer flow region, f_{1s_+},

$$f_{1s_+} = CI - \frac{Ar^4}{64} + \frac{8}{147}Ar^{\frac{7}{2}}\sqrt{r_p} - \frac{1}{18}Ar^3 r_p - \frac{115Ar_p^4}{28224} + \frac{Ar^2 r_p^4}{672R^2(z)} + \frac{1}{12}Ar^2 r_p R(z) - \frac{2}{21}Ar^2 \sqrt{r_p} R^{\frac{3}{2}}(z)$$
$$+ \frac{1}{32}Ar^2 R^2(z) - \frac{1}{336}Ar_p^4 \log(r) + \frac{1}{336}Ar_p^4 \log(r_p), \qquad (45)$$

where $A = \frac{1}{8}\left[-B\frac{dH}{dz} + \frac{dp}{dz}\right]$ and

$$CI = A\left(\frac{13r_p^4}{7056} + \frac{r_p^6}{5280R^2(z)} - \frac{7r_p R^3(z)}{360} + \frac{15\sqrt{r_p}R^{\frac{7}{2}}(z)}{539} - \frac{R^4(z)}{96} - \frac{r_p^4}{336}\log(r_p) + \frac{1}{336}r_p^4 \log(R(z))\right). \qquad (46)$$

The general solution of unsteady dispersion function, $f_{1t}(r,t)$ is given as

$$f_{1t}(r,t) = \sum_{m=1}^{\infty} A_m e^{-\lambda_m^2 t} J_0(\lambda_m r), \qquad (47)$$

where

$$A_m = -\frac{2}{J_0^2(\lambda_m)}\int_0^{R(z)} J_0(\lambda_m r)f_{1s}(r)r\,dr. \qquad (48)$$

The overall dispersion function is given as follows:

$$f_1(r,t) = f_{1s}(r) + f_{1t}(r,t), \qquad (49)$$

where $f_{1s}(r)$ is the steady state dispersion function and $f_{1t}(r,t)$ is the dispersion function in the unsteady state that characterises the solute's time-dependent dispersion. The manuscript does not include the full mathematical formulas for the unsteady and overall dispersion functions due to the expressions are very large which required the use of *Mathematica* to solve.

3. Results and Discussions

The present study goals to investigate the effect of magnetic field on the velocity of Casson fluid and dispersion function by varying the parameters of magnetic field and height of stenosis. The present results of Casson fluid with the effect of magnetic field and height of stenosis are beneficial to depict the non-Newtonian behaviour and the impact of magnetic field and height of stenosis on the velocity and dispersion coefficients.

3.1 Velocity

Figure 2 shows the validation result of velocity, u for the present and previous study in the absence of height of stenosis, a and magnetic field, M with $R(z)=1$, $r_p=0.02$ and $p=4$. The validation figure is found to be in good agreement with Dash *et al.,* [6]. For validation purpose, the geometry of the stenosed artery, $R(z)$ is set to one.
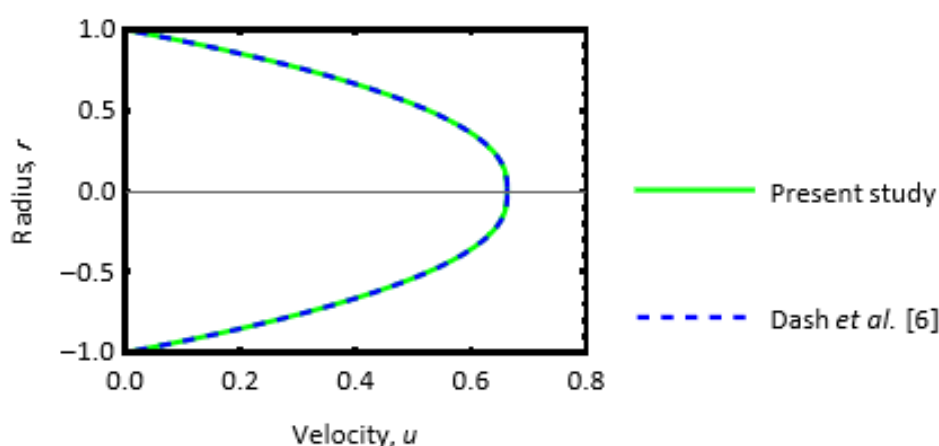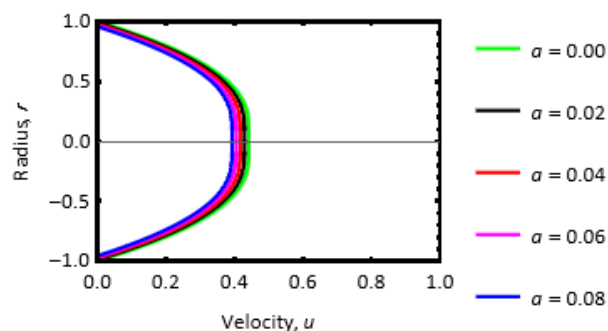

Fig. 2. The validation of velocity of Casson fluid model

Figure 3 shows the variation of velocity for various values of magnetic field, $M=0$, 0.2, 0.4, 0.6, 0.8 when $a=0.02$, $b=2.5$, $z=0.5$, $u_s=0$, $p=4$, $B=1$, $r_p=0.1$ and $dH/dz=1$. The velocity increases, the magnetic field increases. The magnetic force can cause a particle to move in spiral or circular motion which make the velocity increases when it moves through a region of increased magnetic field strength. Thus, the increasing of magnetic field tends to increase the velocity.

Figure 4 shows the variation of velocity of various values of height of stenosis, $a=0$, 0.02, 0.04, 0.06, 0.08 when $M=1$, $b=2.5$, $z=0.5$, $u_s=0$, $p=4$, $B=1$, $r_p=0.1$ and $dH/dz=1$. The velocity decreases as increasing of height of stenosis. This leads to a smaller space for the red blood cells and other cell materials to flow through the artery, hence the decrease in flow velocity. Thus, the velocity decreases when height of stenosis increases.
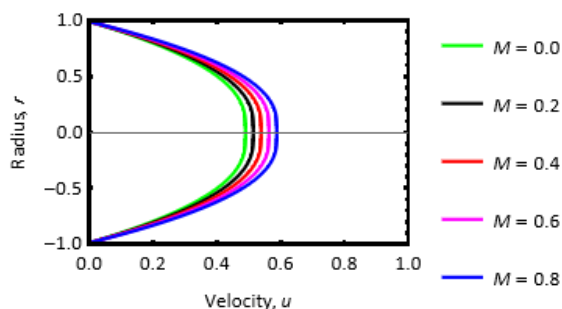
Fig. 3. Velocity of magnetic field, M

Fig. 4. Velocity of height of stenosis, a

3.2 Steady Dispersion Function

Figure 5 shows the validation result of steady dispersion function, f_{1s} for the present and previous study in the absence of height of stenosis, a and magnetic field, M with $R(z)=1$, $r_p=0.02$ and $p=4$. The validation figure is found to be in good agreement with Dash *et al.,* [6]. For validation purpose, the geometry of the stenosed artery, $R(z)$ is set to one.
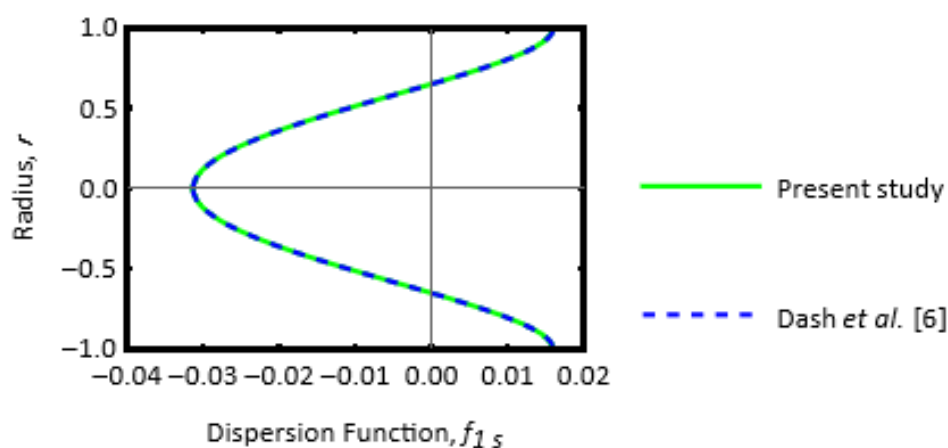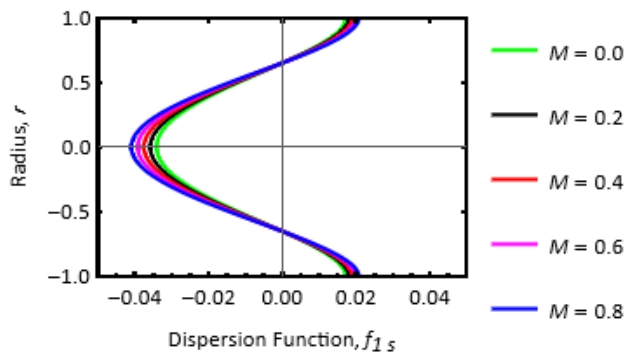

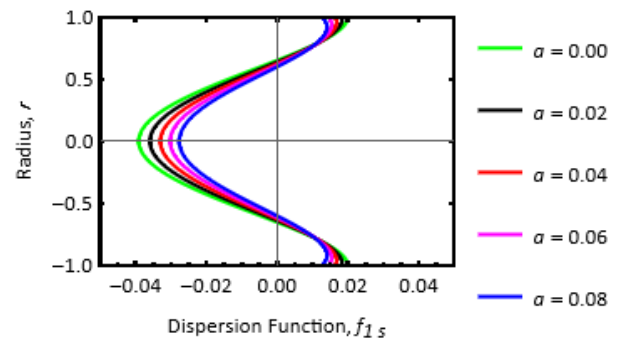**Fig. 5.** Validation of steady dispersion function

Figure 6 shows the variation of steady dispersion function for various values of magnetic field, $M=0$, 0.2, 0.4, 0.6, 0.8 when $a=0.02$, $b=2.5$, $z=0.5$, $u_s=0$, $p=4$, $B=1$, $r_p=0.1$ and $dH/dz=1$. The steady dispersion function decreases, the magnetic field increases. Surface waves in arterial flow destroy cell aggregates due to frequency dispersion, which reduces the inertial/elastic characteristics, while reflection at the artery wall might harm the endothelium sheet and cause denudation, which is the first step in the development of atherosclerosis. It is demonstrable that electromagnetic forces create extra energy in the blood flow. It emerges from the heart's rotating dipole and spreads via ac current to every live cell in the body. Thus, the steady dispersion function decreases when magnetic field increases.

Figure 7 shows the variation of steady dispersion function of various values of height of stenosis, $a=0$, 0.02, 0.04, 0.06, 0.08 when $M=1$, $b=2.5$, $z=0.5$, $u_s=0$, $p=4$, $B=1$, $r_p=0.1$ and $dH/dz=1$. The steady dispersion increases, height of stenosis increases. As stenosis grows larger, the steady dispersion function reduces along the wall, and the opposite behaviour occurs in the artery's core. The scattering function exhibits inverse behaviour under the unstable conditions for

the rheological parameters given above. The height of the stenosis has a significant impact on the size of the stenosis and affects the blood velocity and dispersion process. Thus, steady dispersion function increases when height of stenosis increases.
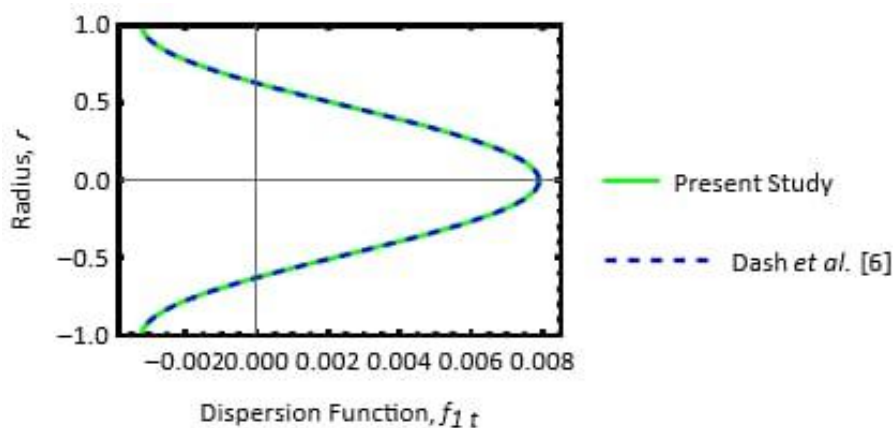

Fig. 6. Steady dispersion function of magnetic field, M

Fig. 7. Steady dispersion function of height of stenosis, a
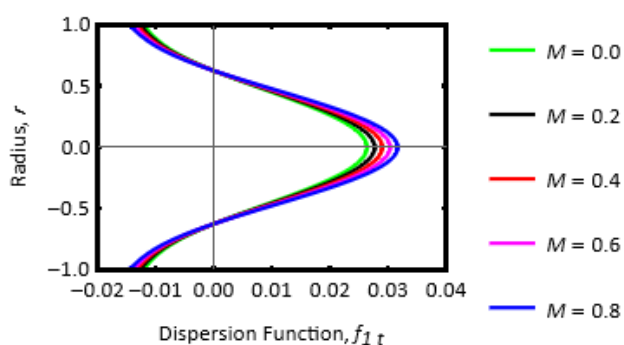
3.3 Unsteady Dispersion Function

Figure 8 shows the validation result of unsteady dispersion function, f_{1t} for the present and previous study in the absence of height of stenosis, a and magnetic field, M with $R(z)=1$, $t=0.5$, $r_p = 0.02$ and $p=4$. The validation figure is found to be in good agreement with Dash *et al.,* [6]. For validation purpose, the geometry of the stenosed artery, $R(z)$ is set to one.
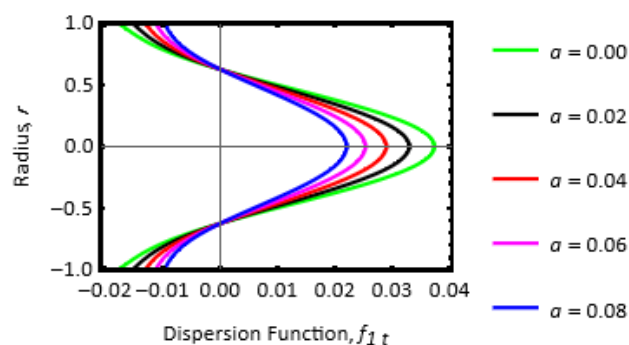

Fig. 8. Validation of unsteady dispersion function

Figure 9 shows the variation of unsteady dispersion function for various values of magnetic field, $M=0$, 0.2, 0.4, 0.6, 0.8 when $a=0.02$, $b=2.5$, $z=0.5$, $u_s=0$, $p=4$, $B=1$, $t=0.01$, $r_p=0.1$ and $dH/dz=1$. The unsteady dispersion function increases, the magnetic field increases. The increasing in magnetic parameters causes a reduction in unsteady dispersion function. Thus, the unsteady dispersion function increases when magnetic field increases.

Figure 10 shows the variation of unsteady dispersion function of various values of height of stenosis, $a = 0$, 0.02, 0.04, 0.06, 0.08 when $M = 1$, $b = 2.5$, $z = 0.5$, $u_s = 0$, $p = 4$, $B = 1$, $t = 0.01$, $r_p = 0.1$ and $dH/dz = 1$. The unsteady dispersion function decreases, height of stenosis increases. As stenosis decreases, the unstable dispersion function increases along the wall and reverses in the artery's core. The scattering function exhibits inverse behaviour under unstable conditions for the rheological parameters given above. Thus, the unsteady dispersion function decreases as increasing of height of stenosis.
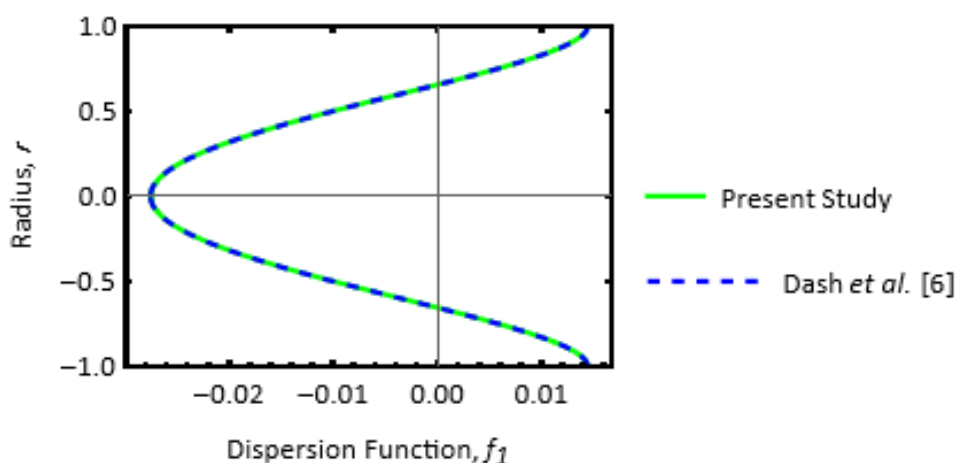

Fig. 9. Unsteady dispersion function of magnetic field, *M*

Fig. 10. Unsteady dispersion function of height of stenosis, *a*
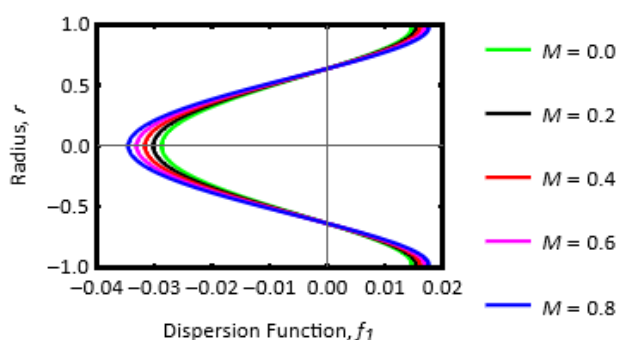
3.4 Overall Dispersion Function

Figure 11 shows the validation result of overall dispersion function, f_1 for the present and previous study in the absence of height of stenosis, a and magnetic field, M with $R(z) = 1$, $r_p = 0.02$ and $p = 4$. The validation figure is found to be in good agreement with Dash *et al.,* [6]. For validation purpose, the geometry of the stenosed artery, $R(z)$ is set to one.
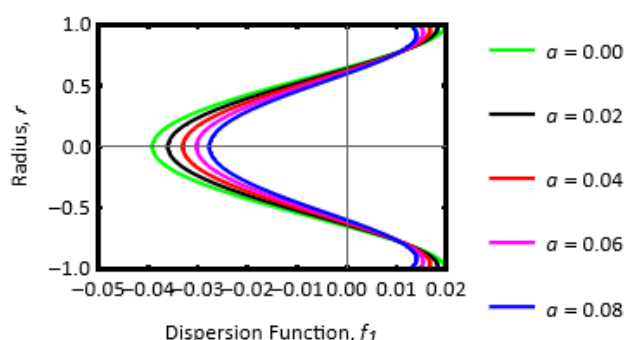

Fig. 11. Validation of overall dispersion function

Figure 12 shows the variation of overall dispersion function for various values of magnetic field, $M = 0, 0.2, 0.4, 0.6, 0.8$ when $a = 0.02$, $b = 2.5$, $z = 0.5$, $u_s = 0$, $p = 4$, $B = 1$, $r_p = 0.1$ and $dH/dz = 1$. The overall dispersion function decreases, the magnetic field increases. The overall dispersion function decreases with the presence of magnetic field since the blood velocity decreases when the magnetic field exists. This is due to the fact that the blood velocity moves together with the overall dispersion function in blood flow. Thus, the overall dispersion function decreases as increasing of magnetic field.

Figure 13 shows the variation of overall dispersion function of various values of height of stenosis, $a = 0, 0.02, 0.04, 0.06, 0.08$ when $M = 1$, $b = 2.5$, $z = 0.5$, $u_s = 0$, $p = 4$, $B = 1$, $r_p = 0.1$ and $dH/dz = 1$. The overall dispersion function increases, the height of stenosis increases. The behaviour of the overall dispersion function is low at the centre of the artery and high at the wall of the artery. However, the increase of overall dispersion function from the centre of the artery to the wall of the artery is uniform in approaching the arterial wall. Thus, the overall dispersion function increases when the height of stenosis increases.

Fig. 12. Overall dispersion function of magnetic field, M

Fig. 13. Overall dispersion function of height of stenosis, a

4. Conclusions

In conclusion, the effect of magnetic field and height of stenosis on the behaviour of steady flow velocity and unsteady solute dispersion through Casson fluid with the presence of stenosed artery can be investigated by manipulating magnetic field and height of stenosis. It can be noted that an increase in magnetic field, increases the velocity and unsteady dispersion function but decreasing in steady and overall dispersion functions. Meanwhile, increasing in height of stenosis, increasing in steady and overall dispersion functions but decreasing in velocity and unsteady dispersion function. The decreases in the flow region that causes red blood cells to flow in a much smaller space leading to an accumulation of red blood cells. Hence, the flow velocity decreases. As for the steady dispersion function, the smaller region caused by the increase in height of stenosis leads to a slower flow velocity and causes the solute to disperse more effectively at a particular region.

As for magnetic field, it leads to a fastest the flow velocity. For unsteady dispersion function, the effect of magnetic field and height of stenosis is reverse behaviour of steady dispersion function. The overall dispersion function is the summation of steady and unsteady dispersion functions. Therefore, the overall dispersion function exhibits similar behaviour to steady dispersion function when magnetic field and height of stenosis increases. The result obtained from the mathematical analysis concluded that the magnetic field and height of stenosis highly influence the velocity flow and dispersion function. Both parameters should be considered when study the dispersion of solute using

Casson fluid model that has a presence of stenosed artery as it changes the behaviour of blood flow and solute dispersion. Therefore, this presence study contributes a significant advancement in the mathematical modelling field of solute dispersion in blood flow through stenosed artery using Casson fluid model.

Acknowledgments

References

[1] Ali, Amjad, Zainab Bukhari, Muhammad Umar, Muhammad Ali Ismail, and Zaheer Abbas. "Cu and cu-swcnt nanoparticles' suspension in pulsatile casson fluid flow via darcy–forchheimer porous channel with compliant walls: a prospective model for blood flow in stenosed arteries." *International Journal of Molecular Sciences* 22, no. 12 (2021): 6494. https://doi.org/10.3390/ijms22126494

[2] Aris, Rutherford. "On the dispersion of a solute in a fluid flowing through a tube." *Proceedings of the Royal Society of London. Series A. Mathematical and Physical Sciences* 235, no. 1200 (1956): 67-77. https://doi.org/10.1098/rspa.1956.0065

[3] Arshadi, Soroosh, and Ahmad Reza Pishevar. "Magnetic drug delivery effects on tumor growth." *Informatics in Medicine Unlocked* 27 (2021): 100789. https://doi.org/10.1016/j.imu.2021.100789

[4] Bell, Caitlin F., Xiudong Lei, Allen Haas, Richard A. Baylis, Hua Gao, Lingfeng Luo, Sharon H. Giordano, Mackenzie R. Wehner, Kevin T. Nead, and Nicholas J. Leeper. "Risk of cancer after diagnosis of cardiovascular disease." *Cardio Oncology* 5, no. 4 (2023): 431-440. https://doi.org/10.1101/2022.08.08.22278548

[5] Das, Prosanjit, Sarifuddin, and Prashanta Kumar Mandal. "Solute dispersion in Casson fluid flow through a stenosed artery with absorptive wall." *Zeitschrift für angewandte Mathematik und Physik* 71, no. 3 (2020): 100. https://doi.org/10.1007/s00033-020-01322-8

[6] Dash, R. K., G. Jayaraman, and K. N. Mehta. "Shear augmented dispersion of a solute in a Casson fluid flowing in a conduit." *Annals of Biomedical Engineering* 28 (2000): 373-385. https://doi.org/10.1114/1.287

[7] Gill, WN-Na5233. "A note on the solution of transient dispersion problems." *Proceedings of the Royal Society of London. Series A. Mathematical and Physical Sciences* 298, no. 1454 (1967): 335-339. https://doi.org/10.1098/rspa.1967.0107

[8] Gill, W. N., and R. Sankarasubramanian. "Exact analysis of unsteady convective diffusion." *Proceedings of the Royal Society of London. A. Mathematical and Physical Sciences* 316, no. 1526 (1970): 341-350. https://doi.org/10.1098/rspa.1970.0083

[9] Jamil, Dzuliana Fatin, Salman Saleem, Rozaini Roslan, Fahad S. Al-Mubaddel, Mohammad Rahimi-Gorji, Alibek Issakhov, and Salah Ud Din. "Analysis of non-Newtonian magnetic Casson blood flow in an inclined stenosed artery using Caputo-Fabrizio fractional derivatives." *Computer Methods and Programs in Biomedicine* 203 (2021): 106044. https://doi.org/10.1016/j.cmpb.2021.106044

[10] Ndenda, J. P., S. Shaw, and J. B. H. Njagarah. "Solute dispersion of drug carrier during magnetic drug targeting for blood flow through a microvessel." *Journal of Applied Physics* 130, no. 2 (2021).. https://doi.org/10.1063/5.0053645

[11] Priyadharshini, S., and R. Ponalagusamy. "Mathematical modelling for pulsatile flow of Casson fluid along with magnetic nanoparticles in a stenosed artery under external magnetic field and body acceleration." *Neural Computing and Applications* 31 (2019): 813-826. https://doi.org/10.1007/s00521-017-3111-8

[12] Sankarasubramanian, R., and William N. Gill. "Unsteady convective diffusion with interphase mass transfer." *Proceedings of the Royal Society of London. A. Mathematical and Physical Sciences* 333, no. 1592 (1973): 115-132. https://doi.org/10.1098/rspa.1973.0051

[13] Senapati, Sudipta, Arun Kumar Mahanta, Sunil Kumar, and Pralay Maiti. "Controlled drug delivery vehicles for cancer treatment and their performance." *Signal transduction and targeted therapy* 3, no. 1 (2018): 7. https://doi.org/10.1038/s41392-017-0004-3

[14] Shahzad, Hasan, Xinhua Wang, Abuzar Ghaffari, Kaleem Iqbal, Muhammad Bilal Hafeez, Marek Krawczuk, and Wiktoria Wojnicz. "Fluid structure interaction study of non-Newtonian Casson fluid in a bifurcated channel having stenosis with elastic walls." *Scientific Reports* 12, no. 1 (2022): 12219. https://doi.org/10.1038/s41598-022-16213-3

[15] Suneetha, S., K. Subbarayudu, and Muhammad Arif. "Theoretical analysis of Casson flow of blood with hybrid magnetic nanoparticles as a drug carrier with magnetic field-Application to treatment of Cancer."

[16] Taylor, Geoffrey Ingram. "Dispersion of soluble matter in solvent flowing slowly through a tube." *Proceedings of the Royal Society of London. Series A. Mathematical and Physical Sciences* 219, no. 1137 (1953): 186-203. https://doi.org/10.1098/rspa.1953.0139

[17] Tzirtzilakis, E. E., and V. C. Loukopoulos. "Biofluid flow in a channel under the action of a uniform localized magnetic field." *Computational Mechanics* 36, no. 5 (2005): 360-374. https://doi.org/10.1007/s00466-005-0659-4

[18] Van Durme, Rikkert, Guillaume Crevecoeur, Luc Dupré, and Annelies Coene. "Model-based optimized steering and focusing of local magnetic particle concentrations for targeted drug delivery." *Drug Delivery* 28, no. 1 (2021): 63-76. https://doi.org/10.1080/10717544.2020.1853281

[19] Verma, Narendra Kumar, Shailesh Mishra, Shafi Ullah Siddiqui, and Ram Saran Gupta. "Effect of slip velocity on blood flow through a catheterized artery." *Applied mathematics* 2, no. 6 (2011): 764. https://doi.org/10.4236/am.2011.26102

[20] Veselov, Valery V., Alexander E. Nosyrev, László Jicsinszky, Renad N. Alyautdin, and Giancarlo Cravotto. "Targeted delivery methods for anticancer drugs." *Cancers* 14, no. 3 (2022): 622. https://doi.org/10.3390/cancers14030622

[21] Wang, Yinghui, Yonggang Wang, Xiaorong Han, Jian Sun, Cheng Li, Binay Kumar Adhikari, Jin Zhang, Xiao Miao, and Zhaoyang Chen. "Cardio-oncology: a myriad of relationships between cardiovascular disease and cancer." *Frontiers in Cardiovascular Medicine* 9 (2022): 727487. https://doi.org/10.3389/fcvm.2022.727487

[22] Yadeta, Habtamu Bayissa, and Sachin Shaw. "Magnetic drug targeting during Casson blood flow in a microvessel: A Caputo fractional model." *Journal of Magnetism and Magnetic Materials* 568 (2023): 170363. https://doi.org/10.1016/j.jmmm.2023.170363